ELSEVIER

Contents lists available at ScienceDirect

Analytica Chimica Acta

journal homepage: www.elsevier.com/locate/aca





Limitations and insights regarding atmospheric mercury sampling using gold

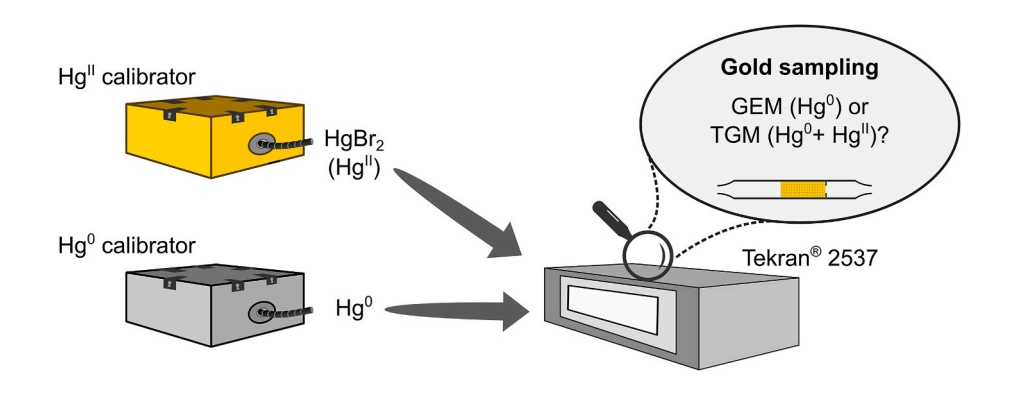
Jan Gačnik ^{a,*}, Seth Lyman ^b, Sarrah M. Dunham-Cheatham ^c, Mae Sexauer Gustin ^a

- ^a Department of Natural Resources and Environmental Science, University of Nevada, Reno, USA
- ^b Bingham Research Center, Utah State University, Vernal, USA
- ^c College of Agriculture, Biotechnology & Natural Resources, University of Nevada, Reno, USA

HIGHLIGHTS

- Gold amalgamation procedure measures a Hg fraction in between Hg⁰ and TGM.
- 10–75 % of Hg^{II} is recovered as Hg⁰ by the Tekran 2537 analyzer.
- Hg^{II} is lost through adsorption and inefficient thermal desorption of Hg from gold.
- Thermolyzer quantitatively converted Hg^{II} to Hg⁰ to enable a TGM measurement.
- Tekran 2537B models measured 1.5 times higher Hg concentrations than 2537X models.

GRAPHICAL ABSTRACT



ARTICLE INFO

Handling Editor: Xiu-Ping Yan

Keywords:
Gaseous elemental mercury
Gold amalgamation
Peak integration algorithm
Permeation calibrator
Tekran 2537 analyzer
Total gaseous mercury

ABSTRACT

Background: Atmospheric mercury (Hg) concentrations are quantified primarily through preconcentration on gold (Au) cartridges through amalgamation and subsequent thermal desorption into an atomic fluorescence spectrometry detector. This procedure has been used for decades, and is implemented in the industry-standard atmospheric Hg analyzer, the Tekran 2537. There is ongoing debate as to whether gaseous elemental mercury (Hg 0) or total gaseous mercury (TGM, Hg 0 + Hg II) is measured using Au cartridges. The raw Hg signal processing algorithms for the Tekran 2537 analyzer have also been questioned. The objective of this work was to develop a better understanding of what forms of Hg are collected on gold cartridges through the use of permeation tube-based calibrators, that release known amounts of Hg 0 and Hg I . The potential differences between different Tekran analyzer models (i.e., 2537B versus 2537X) Hg signal processing algorithms, and Hg 0 calibration methods were also investigated

Results: Experiments were performed using Hg^0 and Hg^{II} permeation calibrators. Validation tests showed that the Hg^{II} calibrator produced a reproducible and stable Hg^{II} permeation rate (2.2 \pm 0.2 pg min⁻¹). Results of Hg^{II} sampling and analysis using Au amalgamation showed the gold cartridges measured up to 75 % Hg^{II} , with the value at the beginning of the Hg^{II} measurement being much lower (as low as 10 %) due to Hg^{II} adsorption on analyzer surfaces and the Tekran particulate filter. Furthermore, thermal desorption of Hg^{II} from Au reduced only 80 % of Hg^{II} to Hg^0 , resulting in additional Hg^{II} that was not measured by the analyzer. By adding a thermolyzer

E-mail address: jan.gacnik@ijs.si (J. Gačnik).

^{*} Corresponding author.

upstream of the analyzer, 97 % of Hg^{II} was measured as Hg^0 . Additionally, Hg^0 measurements using Tekran 2537 B and X models using a newly developed signal processing algorithm, different peak integration methods, and two Hg^0 sources were compared. Results showed the 2537X model was not affected by the integration type, while the 2537B model was. Bell jar calibration based on the Dumarey equation resulted in 6 % \pm 7 % (mean \pm SD) underestimation of measured Hg^0 concentrations compared to the calibration with a permeation calibrator. Significance: Gold cartridges measured an atmospheric Hg fraction somewhere between Hg^0 and Hg due to Hg^{II} adsorption and inefficient reduction of Hg^{II} to Hg^0 during thermal desorption from Au. Since Hg^{II} in ambient air can be 25 % of total Hg, distinguishing between Hg^0 and Hg^0 is important. The use of a thermolyzer or a cation exchange membrane upstream of gold cartridges is recommended to enable Hg^0 or Hg^0 measurements, respectively. Observations showed that traceable multipoint calibrations of atmospheric Hg^0 measurements are needed for Hg^0 quantification, and that different Hg^0 calibration methods can produce significantly different results for measured atmospheric Hg^0 concentrations.

1. Introduction

Amalgamation of mercury (Hg) and gold (Au) has been used since the 11th century for extracting Au from ore [1]. The principle of amalgamation of Hg and Au has also been applied in analytical chemistry. For example, widespread use of Hg amalgamation on Au sorbents for Hg analysis began in the late 1960s [2–4]. A Au wire sorbent was the first material applied for atmospheric Hg measurements [4]. In addition to Au wire, other variants of Au materials have been used to measure Hg, including Au nanostructures and high surface-area substrates coated with Au [5]. Cartridges containing Au-coated quartz are currently the most commonly used sorbent material for atmospheric Hg sampling and analysis, frequently referred to as "Au cartridges". Au cartridges are used in the current industry standard atmospheric Hg analyzer, the Tekran Instrument Corporation's 2537 Hg vapor analyzer (hereafter referred to as "the Tekran analyzer").

Atmospheric Hg consists of gaseous elemental mercury (Hg⁰, GEM), gaseous oxidized mercury (HgII, GOM), and particulate-bound mercury (Hg-p, PBM). Total gaseous mercury (TGM) is defined as $Hg^0 + Hg^{II}$. Most of the current analytical challenges are related to HgII and Hg-p measurements, as they are reactive and usually present at low pg m concentrations in ambient air [6], compared to much higher Hg⁰ concentrations that are typically 1–2 ng m⁻³. Nevertheless, uncertainties also exist for ${\rm Hg^0}$ and TGM measurements, even after more than 50 years of atmospheric Hg measurements. During the Tekran analyzer standard operating procedure, ambient air is drawn through Au cartridges to preconcentrate atmospheric Hg, followed by thermal desorption in argon carrier gas and detection of Hg⁰ using cold vapor atomic fluorescence spectrometry (CVAFS) [7]. The uncertainty of raw Hg CVAFS signal processing has been previously investigated, and studies showed that improved peak integration algorithms can promote better comparability of Hg⁰ and TGM measurement results obtained with different Tekran analyzers [8-10]. However, further work on integration algorithms is needed. One of the biggest uncertainties in atmospheric Hg⁰ and TGM measurements is whether sampling and analysis using an Au cartridge results in a Hg⁰ measurement, a TGM measurement, or somewhere in between. The topic is still a matter of debate, without conclusive experimental results [11-13]. Processes occurring during sampling and analysis of gaseous Hg^{II} with the Tekran analyzer are not well understood, although it is known that any Hg^{II} potentially reaching the CVAFS is not detected at the wavelength used by the analyzer (253.7 nm) [14]. Furthermore, Hg⁰ measurements using collocated instruments from the same manufacturer can differ by up to 30 % [12,15], raising questions about the comparability of measurement data. The comparability of atmospheric Hg measurement data is crucial in the light of the Minamata Convention on Mercury, ratified in 2013. The Convention, established by the international community, aims to reduce anthropogenic emissions and releases of Hg into the environment.

Studies of gaseous Hg^{II} have been limited by the unavailability of reliable Hg^{II} calibration sources. However, recent advances in Hg^{II} permeation sources [16,17] and introduction of new Hg^{II} sources, such as a source based on nonthermal plasma oxidation [18], allow new

insights into gaseous $\mathrm{Hg^{II}}$ behavior. The objective of this work was to use improved Hg sources to enhance our understanding of atmospheric Hg analyzers, ultimately aiming to improve the quality of atmospheric Hg monitoring—an essential aspect for evaluating the effectiveness of the Minamata Convention. To this end, a newly developed $\mathrm{Hg^{II}}$ permeation calibrator was validated and used to better understand the processes occurring during Au cartridge sampling of gaseous $\mathrm{Hg^{II}}$ and during typical operational conditions of the Tekran 2537 analyzer. Additionally, a real-time peak height calculation algorithm was developed that can be used with legacy Tekran 2537 analyzers (Tekran 2537A and 2537B) that do not have a peak height calculation option. The developed algorithm was used to conduct experiments to simultaneously compare: i) peak area and peak height integration; ii) bell jar and permeation calibrator $\mathrm{Hg^0}$ calibration; and iii) Tekran 2537B and Tekran 2537X analyzers.

2. Materials and methods

2.1. Hg permeation calibrators

Hg^{II} calibrations were performed with a custom-built permeation tube-based calibrator. Some components of the calibrator were based on previous designs [15-17]. All tubing and fittings in the calibrator that were exposed to HgII were constructed of stainless steel coated with deactivated fused silica (Sulfinert by SilcoTek Corporation). The calibrator used an HgBr2 permeation tube, constructed from 0.2 mm polytetrafluoroethylene (PTFE) tubing as described in Ref. [17]. The tube was housed in a 5 mm inner diameter tube, and ultra-high purity helium (He), controlled by a 7 µm flow orifice, flowed across the permeation tube at 10 mL min⁻¹. The permeation tube housing was kept within an insulated aluminum block at 50 \pm 0.05 °C. The HgBr $_2$ permeation tube was allowed to equilibrate at its set temperature for at least 48 h before use. After the housing, Hg and He passed through a 1 mm inner diameter tube of 10 cm length, through a zero dead volume tee (Valco Instruments Company Incorporated), and into a 2 mm inner diameter tube of 30 cm length. Ambient air that passed through an iodated carbon scrubber and a $0.2~\mu m$ filter was added at the zero dead volume tee and controlled with a mass flow controller to create a total flow of 200 mL min⁻¹. After the 2 mm inner diameter tube, the gas mixture passed through a custom Venturi-type flow meter. The flow meter consisted of a 5 cm length of 1 mm inner diameter tubing followed by a 5 cm length of 0.5 mm inner diameter tubing, followed by an outlet line that consisted of a 0.5 mm inner diameter tube of 1.2 m length. The lengths of tubing were connected with zero dead volume tees, and differential pressure was measured at the two downstream-most tees. The flow rate was determined from the differential pressure measurement by linear regression with results from a NIST-traceable Bios DryCal flow meter. All tubing after the aluminum block, including the flow meter, was insulated and heated to 150 \pm 1 $^{\circ}\text{C}.$

 ${\rm Hg}^0$ calibrations were performed with the calibrator described by Dunham-Cheatham et al. [15]. Briefly, it was similar to the ${\rm Hg}^{II}$ calibrator described above, except (1) it contained several permeation

tubes, and a VICI gas chromatography valve was used to select among the tubes, (2) it contained a second gas chromatography valve that allowed for selection between two available outlet lines, (3) permeation tubes were heated to 70 \pm 0.05 °C, (4) high-purity N_2 was used as the carrier gas, flow orifices were coated with Sulfinert® and placed downstream of permeation tubes to ensure the tubes were under constant pressure, (5) the permeation oven was configured differently (see Dunham-Cheatham et al. for details), and (5) all components after the permeation oven were heated to $140\pm1~^\circ\text{C}.$

2.2. Calibrator validation tests

The experiments conducted in this work depended on the well-characterized permeation rate of the ${\rm Hg}^{\rm II}$ and ${\rm Hg}^{\rm O}$ calibrators. Validation of the ${\rm Hg}^{\rm O}$ calibrator was done in previous work [19]; the ${\rm Hg}^{\rm O}$ permeation rate was determined to be 10.9 pg s⁻¹. Therefore, validation tests were performed for the ${\rm Hg}^{\rm II}$ calibrator to determine ${\rm Hg}^{\rm II}$ (Fig. 1A) and ${\rm Hg}^{\rm O}$ permeation rates from its ${\rm HgBr}_2$ permeation tube (Fig. 1B).

The permeation rate of Hg^{II} was tested by connecting the calibrator outlet to a filter pack containing cation exchange membranes (CEM; Pall Corporation, Mustang S; 0.8 μ m pore size). CEM were used as they were previously shown to capture Hg^{II} quantitatively, while not retaining Hg^{0} [20]. Additionally, CEM outperformed other alternative membrane surfaces tested for Hg^{II} retention [21]. The stability of the Hg^{II}

permeation rate was tested by loading CEM at different times during 24 h of continuous calibrator operation. Reproducibility was tested by comparing permeation rates obtained on different days over a span of 3 months of calibrator tests. CEM were loaded for 10 min at 1 L min⁻¹ flow; the target amount of Hg^{II} loaded on the CEM was ~ 1 ng. The calibrator outlet was inserted directly into the filter cartridge around 2 cm away from the CEM to minimize potential HgBr₂ adsorption to the filter cartridge. The connection between the filter cartridge and the calibrator outlet was not airtight to prevent pressure issues within the calibrator that could cause instabilities in the HgBr2 permeation rate. Consequently, a small amount of HgII and Hg-p (negligible in comparison to the Hg^{II} permeating from the calibrator) was drawn through the membranes from the laboratory air. This was accounted for by subtracting method blanks made by drawing laboratory air through the filter cartridge without exposure to the flow of HgBr₂ from the calibrator and doing so for the same amount of time as the duration of the experiment [21]. Typically, at least 3 CEM were used for method blanks and at least 3 CEM were loaded with Hg^{II} at the start and at the end of each experimental day (6 CEM in total). The mean Hg^{II} permeation rate was then obtained by averaging HgII permeation rates observed on 7 different days (n = 25 total).

The permeation rate of Hg^0 from the Hg^{II} calibrator was tested in two steps. In the first step (loading step), an airtight connection was made between the Hg^{II} calibrator and a CEM cartridge. Downstream of the

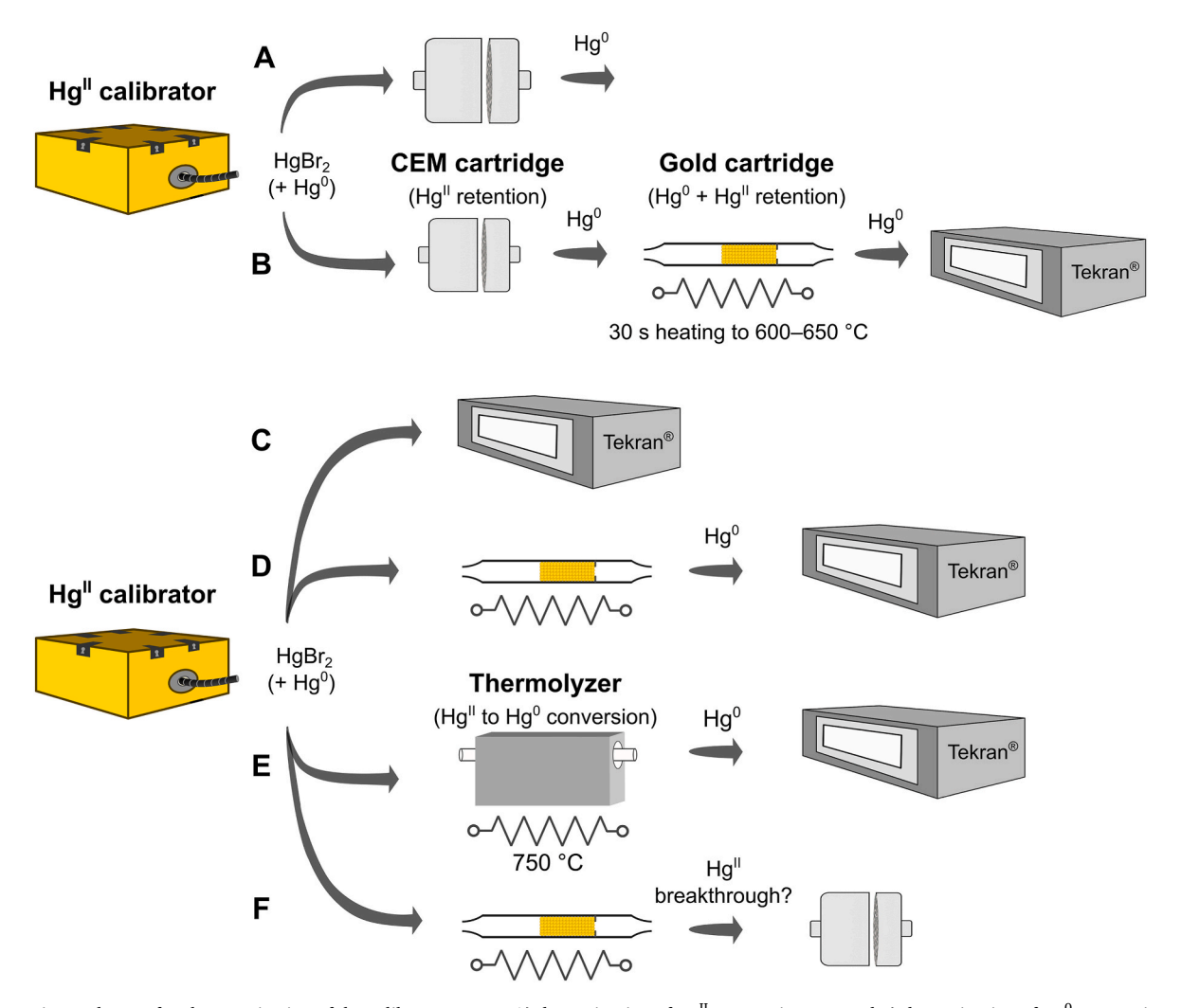


Fig. 1. Experimental setup for characterization of the calibrator output: A) determination of Hg^{II} permeation rate and B) determination of Hg⁰ permeation rate from the Hg^{II} calibrator. Experimental setup for Au sampling tests: C) direct loading of Hg^{II} into the Tekran analyzer, D) loading of Hg^{II} into an external Au cartridge followed by Hg⁰ measurement using the Tekran analyzer, E) loading of Hg^{II} into thermolyzer and subsequent analysis of Hg⁰ using the Tekran analyzer, and F) evaluation of Hg^{II} breakthrough for the Au cartridges. All CEM were analyzed according to EPA method 1631 Revision E.

CEM, an Au cartridge (Tekran part number 35-26510-00) was connected. The flow rate of 0.2 L min⁻¹ was driven by the calibrator. Hg^{II} was retained by the CEM, while Hg⁰ passed through the CEM and was retained on the Au cartridge. Loading was carried out for 3 min to ensure sufficient Hg^0 on the Au cartridge for analysis. Before and after each loading, the Au cartridge was heated in zero (Hg-free) air connected to the Tekran 2537X to confirm that there was no Hg leftover on the cartridge (<1 % of the loaded Hg amount), therefore blanks were not subtracted. In the second step, the downstream Au cartridge was transferred to a Hg-free line with scrubbed air using a charcoal filter, and Hg⁰ was released from the Au cartridge in the vacuum flow of 1 L min⁻¹ (controlled by the Tekran vacuum pump) by coil heating (30 s ramp heating to 600–650 $^{\circ}$ C, simulating the procedure used by the Tekran analyzer). The released Hg⁰ was measured using a Tekran 2537X. The whole procedure was repeated 10 times. An external Au cartridge was used to enable a two-step procedure, required due to a flow rate and pressure mismatch between the calibrator and the Tekran analyzer. The external Au cartridge was calibrated using bell jar Hg⁰ injections based on the Dumarey equation [22]. The bell jar was kept at 20 °C that was also room temperature, to avoid errors due to temperature differences. Best practice guidelines outlined in Brown & Brown [23] and Tekran® 2537 manuals [7] were followed for bell jar injections to minimize the potential biases in injected Hg⁰ concentration. There was no statistically significant difference between the external Au cartridge Hg⁰ injections and Hg⁰ injections directly into the Tekran® 2537X analyzer (*t*-test, p > 0.05). The same calibration procedure was performed for all external Au cartridges used in this work.

2.3. Au sampling tests

The HgII permeation calibrator and Tekran 2537X analyzer were used for all experiments described in this section. First, the Hg^{II} permeation calibrator was connected directly to the Tekran analyzer and the experiment was conducted continuously for approximately 2 days (Fig. 1C). During the 5-min sampling intervals used by the Tekran analyzer, 90 pg of HgII was permeated from the calibrator (at a sampling flow rate of 1 L min⁻¹, this is equivalent to the expected concentration of 18 ng Hg^{II} m⁻³ measured by the Tekran analyzer). Due to the flow rate and pressure mismatch between the calibrator and the Tekran analyzer, the connection between the two instruments was not airtight. Therefore, laboratory air was drawn into the Tekran analyzer in addition to the permeated Hg, meaning that subtraction of laboratory air Hg concentration was needed. Laboratory air Hg concentration was measured for 50 min with the Tekran analyzer before and after the experiment to ensure the concentration was stable. The mean value and relative standard deviation for the laboratory air Hg concentration during the experiment were 5.6 ng m^{-3} and 4 %, respectively.

During the direct continuous injection experiment (Fig. 1C), adsorption losses of ${\rm Hg^{II}}$ were identified (a discussion of ${\rm Hg^{II}}$ adsorption available in the Results and Discussion section), and therefore, additional experiments were conducted with an external Au cartridge to eliminate the ${\rm Hg^{II}}$ adsorption losses (Fig. 1D). Adsorption of ${\rm Hg^{II}}$ was eliminated by minimizing the distance (<2 cm) between the calibrator outlet and the external Au cartridge. The experiment was carried out in two steps. First, the external cartridge was loaded with ${\rm Hg^{II}}$ using the calibrator. In the second step, the external Au cartridge was transferred to the Hg-free line and Hg was released from the external Au cartridge by coil heating (30 s ramp heating to 600–650 °C, simulating the procedure used by the Tekran analyzer). The released Hg was measured using the Tekran analyzer.

Thermolyzers have previously been applied in dual-channel systems for atmospheric Hg analysis [15,17,24]. Thermolyzers can reduce gaseous $\mathrm{Hg}^{\mathrm{II}}$ to Hg^{0} upstream of the Tekran analyzer, potentially enabling TGM measurements and eliminating issues with adsorption and incomplete thermal reduction of $\mathrm{Hg}^{\mathrm{II}}$ to Hg^{0} . Thermolyzer tests were conducted by permeating $\mathrm{Hg}^{\mathrm{II}}$ from the calibrator directly into the

thermolyzer that was connected to a downstream Tekran analyzer (Fig. 1E). Again, the connection between the calibrator and the thermolyzer was not airtight, due to a flow rate and pressure mismatch. The subtraction of laboratory air Hg concentration was performed in the same way as described for the direct continuous injection experiment.

The ability of Au cartridges to quantitatively retain Hg^{II} was tested using the experimental design shown in Fig. 1F. The calibrator outlet was connected to an external Au cartridge with a downstream filter pack containing CEM. The downstream CEM would retain Hg^{II} that passed through the Au cartridge due to inefficient Hg^{II} retention. Loading was carried out for 10 min to ensure that the amount of Hg^{II} on the CEM that potentially passed through the Au cartridge was sufficient for further analysis.

For all Au sampling tests, the recovery of Hg^{II} was determined using equation (1):

Recovery of
$$Hg^{II} = \frac{Measured Hg^{II} concentration}{Theoretical Hg^{II} concentration}$$
 (1)

Measured Hg^{II} concentration was the Hg^{II} concentration either measured by the Tekran analyzer (Fig. 1C, D, and E) or by membrane analysis (Fig. 1F). Theoretical Hg^{II} concentration was the Hg^{II} concentration calculated based on the known permeation rate of Hg^{II} determined in the calibrator validation tests.

2.4. Comparison of peak integration types and Tekran 2537 analyzer

The latest Tekran analyzer model (model 2537X) uses a built-in peak area or peak height integration option for CVAFS signal processing. However, both integration options cannot be used simultaneously for the same sample measurement, and require recalibration after changing the integration type. Older models (i.e., models 2537A and 2537B) only use the peak area integration option [7]. Therefore, a signal processing algorithm was developed that allows simultaneous peak area and peak height integration for 2 different models of Tekran analyzers (2537B and 2537X) operating simultaneously. The algorithm was the same as used by Lyman et al. [17], and was programmed in CRBasic for a CR1000X data logger. The 2537 analyzers were set to output the detector signal to the CR1000X at 0.1 s intervals. The CRBasic program calculated the average signal at the beginning and end of the signal stream and calculated a linear regression slope for the signal baseline. The signal was detrended based on the baseline linear regression. The program then found the maximum signal and calculated the difference between the maximum and the expected baseline at the point of maximum signal. This value was the peak height. The peak height calculated this way was strongly correlated with peak height calculated internally by the 2537X $(r^2 > 0.99).$

The comparison experiment was conducted by varying three different experimental conditions (as shown in Fig. 2 and Fig. S1): i) instrument model (Tekran 2537B and 2537X analyzers), ii) CVAFS signal processing type (peak area and peak height integration), and iii) Hg⁰ source (permeation calibrator and bell jar). Injections using the Hg⁰ permeation calibrator were performed by manually inserting the calibrator outlet into the sample line of Tekran analyzers for a set amount of time. Injection times from 2 to 50 s were used to obtain 5 different concentration points. Syringe injections of Hg⁰ from the bell jar were performed manually by inserting the syringe into the sample line of the Tekran analyzers. Injection volumes from 2.5 to 50 µL, equivalent to 34–659 pg Hg⁰, were used to obtain 5 different concentration points. The bell jar was kept at 20 °C that was also room temperature, to avoid biases due to temperature differences, as described in detail in Brown & Brown [23]. In general, best practice guidelines outlined in Brown & Brown [23] and Tekran 2537 manuals [7] were followed for bell jar injections to minimize the potential biases in injected Hg⁰ concentration. The multipoint calibration curves obtained from the bell jar Hg⁰

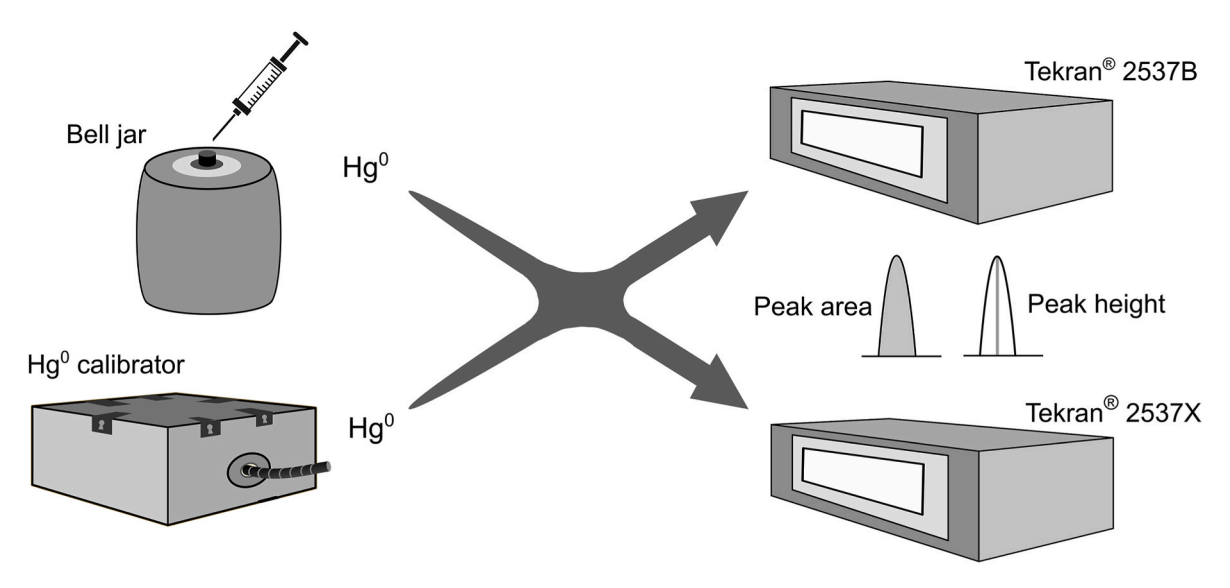


Fig. 2. Experimental variations for the comparison experiments. Peak area and height were measured simultaneously for each analyzer. The whole experimental variation shown in the figure was repeated for 2 sets of Tekran analyzers (4 analyzers were used in total, with two 2537B and two 2537X analyzers).

injections were used to calculate the expected Hg⁰ concentration for injections using the Hg⁰ permeation calibrator for each Tekran 2537 model. A typical analytical sequence used for the comparison experiment is shown in Table S1. Again, the connection between the calibrator and the Tekran analyzers was not airtight due to a flow rate and pressure mismatch. Subtraction of laboratory air Hg concentration was performed in the same way as described in section 3 of materials and methods. The mean value and relative standard deviation for the laboratory air Hg concentration during the experiments were 6.4 ng m⁻³ and 2 %, respectively. At the end of the analytical sequence, syringe injections of Hg⁰ from the bell jar into the zero air line of the analyzer were also carried out to confirm that there was no statistically significant difference between the results obtained by subtracting the laboratory air Hg concentration and the zero air results (t-test, p > 0.05; for both peak area and peak height). The comparison experiment was conducted twice using two different pairs of 2537B and 2537X analyzers (a total of 4 analyzers were used, two 2537B analyzers and two 2537X analyzers) to eliminate the possibility of a potential analyzer malfunction affecting the comparison results. After finishing the comparison experiments, 3 out of 4 analyzers used in the comparison were used for measurements of laboratory air Hg concentrations (Fig. S2). Laboratory air Hg concentrations were relatively stable (4.5 \pm 0.5 ng $\mbox{m}^{-3},$ average of all analyzers \pm SD) and low in comparison to the Hg^0 concentrations injected by the bell jar and permeation calibrator (8–240 $\mathrm{ng}\ \mathrm{m}^{-3}$). Therefore, the deviation of laboratory air Hg concentration presented 0.2–7% of the injected Hg⁰ concentrations. We note that the laboratory air Hg measurements were not conducted in the same period as the comparison experiments, thus the conditions may be different than when comparison experiments were conducted, though the room is isolated and Hg concentrations are relatively stable over long time periods, as previously measured (data not shown). Overall, the laboratory air Hg measurements further confirmed that subtracting the laboratory air Hg concentration did not affect comparison results.

When comparing the bell jar and permeative calibrator results, equations (2)–(4) were used to calculate the difference between the two ${\rm Hg}^0$ sources:

Relative difference =
$$\frac{h_{\text{bell jar}} - h_{\text{calibrator}}}{h_{\text{calibrator}}}$$
 (2)

$$h_{\text{bell jar}} = \frac{h_{\text{bell jar,raw}} - \overline{h}_{\text{laboratory}}}{C_{\text{bell jar}} V_{\text{injection}}}$$
(3)

$$h_{\text{calibrator}} = \frac{h_{\text{calibrator,raw}} - \overline{h}_{\text{laboratory}}}{p_{\text{calibrator}} t_{\text{injection}}}$$
(4)

Where: $h_{\text{bell jar}}$ is the peak height signal normalized to the mass of Hg^0 from the bell jar $[pg^{-1}]$; $h_{\text{calibrator}}$ is the peak height signal normalizeded to the mass of Hg^0 from the permeative calibrator $[pg^{-1}]$; $h_{\text{bell jar, raw}}$ is the raw peak height signal for the bell jar Hg^0 ; $h_{\text{calibrator, raw}}$ is the raw peak height signal for the permeative calibrator Hg^0 ; $\overline{h}_{\text{laboratory}}$ is the mean raw peak height signal for the laboratory air Hg; $C_{\text{bell jar}}$ is the concentration of Hg^0 in the bell jar $[pg \, \mu L^{-1}]$; $V_{\text{injection}}$ is the volume of air drawn from the bell jar with a syringe $[\mu L]$; $p_{\text{calibrator}}$ is the Hg^0 permeation rate of the permeative calibrator $[pg \, s^{-1}]$; $t_{\text{injection}}$ is the time of injection for the permeative calibrator [s]. Raw peak height values normalized to the mass of injected Hg^0 were used in equations (3) and (4) to avoid any potential biases from the internal Tekran calibration.

2.5. Membrane analyses, Tekran analyzer measurements, and data processing

Total Hg content on CEM was determined using a revised (5.66% BrCl) EPA Method 1631 Revision E [25] and subsequent CVAFS using a Tekran 2600-IVS. For more details about the analytical method for CEM, see Supplementary material (Text S1).

Tekran 2537B (two analyzers) and 2537X (two analyzers) were operated at a sampling flow rate of 1 L min $^{-1}$ and 2.5 min sampling cycles. Complete lists of instrument parameters for both analyzer types are available in Supplementary material (Text S2). The upstream PTFE membrane (Sartorius Stedium Biotech, 1180747 N; 0.2 μ m pore size) for particle removal was changed once per week or after experiments exposing PTFE membranes to high Hg^{II} concentrations. The analyzers were calibrated using the internal Hg^0 calibration source at the start of every experimental day. Additionally, the recovery was checked by performing 6–10 manual injections of Hg^0 from a bell jar at the start and end of each experimental day. The detector voltage was kept at $\sim\!0.1\pm0.01$ V, while the baseline deviation remained below 100 mV. All analyzers were checked for leaks in the sample lines and argon lines.

Statistical tests, data processing, and data visualization were performed in R, version 4.2.1 [26]. Friedman tests (non-parametric repeated measures analysis of variance by ranks) were used to test the statistical similarity of the results for two different Tekran Au cartridges used for the direct continuous injection test. Friedman tests were used to test the statistical similarity of comparison data obtained by different

Tekran 2537 analyzer models. Statistical similarity for external Au cartridge data was tested using Kruskal-Wallis tests (non-parametric one-way analysis of variance by ranks). T-tests were used to test the statistical similarity of the results obtained with subtraction of ambient air Hg concentrations, the results obtained with zero air, and for comparison of peak integration types, Tekran 2537 analyzer models, and Hg⁰ sources. RStudio code for Friedman and Kruskal-Wallis tests is available in Supplementary material (Text S3 and S4, respectively). Creation and editing of the graphical abstract and figures were done in Inkscape, version 1.2.1.

3. Results and discussion

3.1. Hg^{II} calibrator validation results

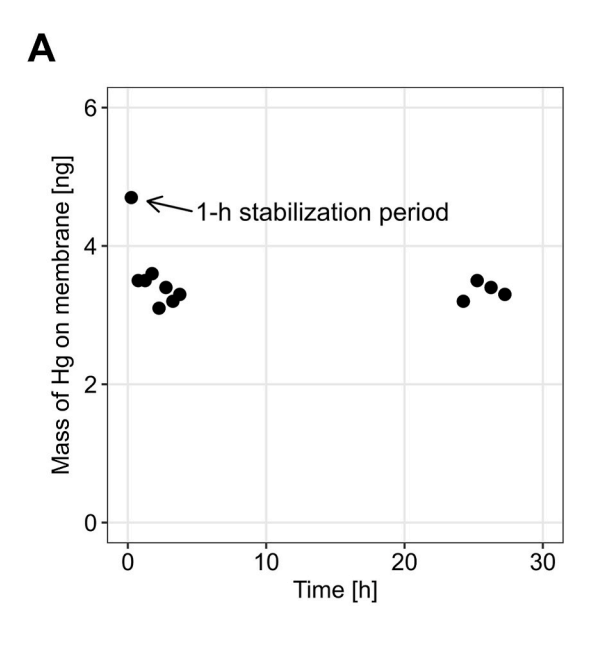
The permeation rate of HgII (as HgBr₂) was stable, with the exception of the first time point (Fig. 3A). The first time point was an outlier, because the permeation calibrator required approximately 1 h to equilibrate and reach a stable HgII output. All future tests using the calibrator were conducted to include a minimum of 90 min of equilibration time prior to running experiments using the calibrator. The longterm Hg^{II} permeation rate evaluated over 3 months of calibrator validation experiments was determined at 2.2 \pm 0.2 pg s⁻¹ (mean of means \pm standard deviation of the mean; n = 7) (Fig. 3B). The permeation rate of ${\rm Hg}^0$ from the ${\rm Hg}^{\rm II}$ calibrator was determined at 0.13 \pm 0.01 pg s⁻¹ (mean \pm standard deviation; n = 10). Therefore, the Hg⁰/Hg^{II} ratio in the Hg^{II} calibrator output was 6 %. Literature values for Hg⁰/Hg^{II} ratios of different permeation-based Hg^{II} sources vary by the design of the source [27], with the ratio ranging from <10% [20,28,29] and up to 70 % [29]. The ratio obtained in our work is at the low end of ratios observed in the literature. Low Hg^0/Hg^{II} ratios are advantageous since Hg^{II} should be the main form of Hg in the output of Hg^{II} calibrators. In all subsequent Au sampling tests, the Hg^{II} and Hg^0 permeation rates determined in the validation tests were taken into account when calculating the results obtained with the ${\rm Hg}^{\rm II}$ calibrator.

3.2. Au sampling results

The stable and reproducible Hg^{II} permeation rates combined with a low Hg^0/Hg^{II} ratio provided the necessary validation data to perform subsequent Au sampling tests.

The results of direct continuous injection of HgII into the Tekran analyzer are shown in Fig. 4A. The recovery of Hg^{II} at the beginning of the experiment was as low as 10 %. Over the course of the experiment, the recovery increased steadily until reaching a plateau of 75 % after 40 h of continuous Hg^{II} injection. The spike in recovery values during hours 38 and 39 was most likely the result of an unaccounted spike in laboratory Hg concentration. The increase in HgII recovery over time was due to adsorption of HgII on tubing and surfaces in the Tekran analyzer before Hg^{II} reached the Au cartridge. This occurrence is in line with the results obtained by Ref. [30], who observed a similar time-dependent increase in Hg^{II} recovery when using an evaporative Hg^{II} calibrator in combination with impinging solutions for Hg^{II} sampling. The sampling line length during our experiment was minimized, therefore, the only line that could provide a surface for HgII adsorption was inside of the Tekran analyzer. Additionally, the analyzer uses a PTFE filter upstream of the sample line to remove particulate matter; the PTFE filter provides additional surface area for ${\rm Hg^{II}}$ adsorption, as shown in the work of Allen et al. [21]. After 40 h of continuous Hg^{II} injection, surfaces were saturated with adsorbed Hg^{II} and Hg^{II} recovery no longer increased, similar to what was previously observed [30]. Interestingly, the recovered Hg^{II} was statistically different for the two Tekran Au cartridges (cartridges A and B) (Friedman, p < 0.05), which can be attributed to the fact that the sample line within the analyzer is split into two lines, one for each Au cartridge. Concerning real-time atmospheric Hg measurements, the above results do not significantly affect the TGM measurements if the relative proportion of Hg^{II} in ambient air is small. On the other hand, for sampling sites with elevated Hg^{II} concentrations and sites exhibiting sudden spikes of Hg^{II} concentration, the results from Fig. 4A imply that TGM measurements would be underestimated due to a dampening effect on measured Hg^{II} concentration. It is important to note that Hg^{II} concentrations have been shown to be up to 25 % of ambient Hg air concentrations [31,32].

The cause of the missing percentage of recovered Hg^{II} even after 40 h



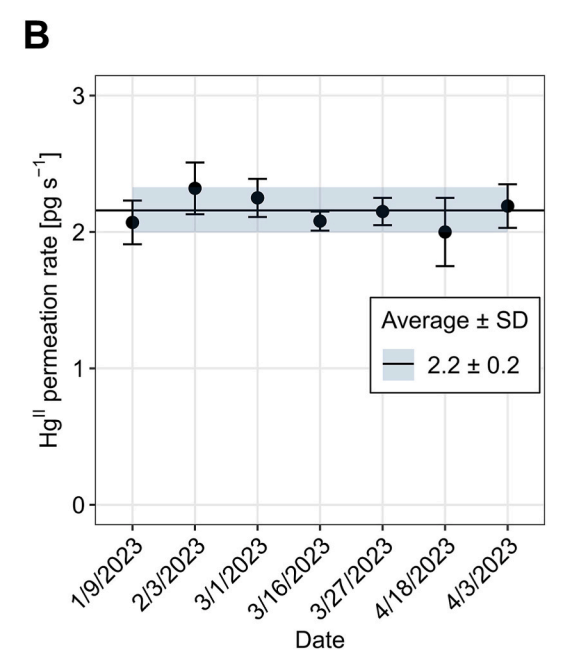


Fig. 3. Hg^{II} calibrator validation results: A) stability of Hg^{II} permeation rate during continuous calibrator operation; and B) long-term reproducibility of the Hg^{II} permeation rate. In B), the black line with corresponding standard deviation were obtained by averaging Hg^{II} permeation rates observed on 7 different experimental days (mean of means \pm SD of the mean, each daily mean representing minimum 3 replicate measurements).

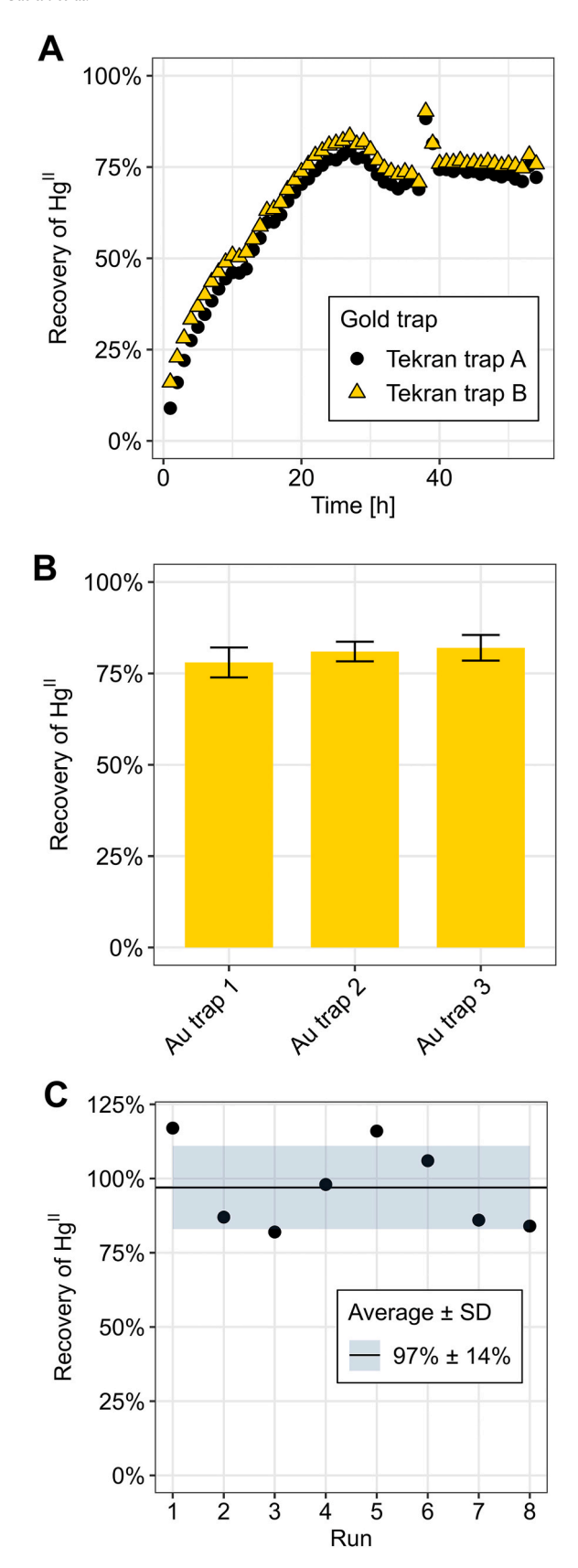


Fig. 4. Au sampling results: A) direct continuous injection of Hg^{II} into the Tekran 2537 analyzer; B) injection of Hg^{II} onto an external Au cartridge; and C) injection of Hg^{II} into a thermolyzer with a downstream Tekran 2537X analyzer.

of direct continuous injection of HgII into the Tekran analyzer was investigated using an external Au cartridge where the adsorption of HgII could be minimized. The results of the external Au cartridge experiments are shown in Fig. 4B. The recovery of Hg^{II} was higher in comparison to Fig. 4A, which was due to minimized adsorption losses of HgII. There was no statistically significant difference between the results obtained with different external Au cartridges (cartridges 1, 2, and 3; Kruskal-Wallis, p > 0.05), confirming that the results were not an outcome of a malfunctioning Au cartridge. The mean recovery for all experiments (n = 27) was 80 \pm 4 % (mean \pm SD). This mean recovery is similar to the recovery obtained after 40 h of continuous HgII injection (Figs. 4A and 75 \pm 2 %; mean \pm SD for all data points after hour 40). The similarity of the two recovery values indicates that adsorption was indeed the reason for the low results in the first 40 h of direct continuous injection test, as hypothesized in the previous paragraph. The missing 20-25 % of recovered Hg^{II} can be attributed to inefficiency of Hg^{II} to Hg⁰ thermal reduction during Au cartridge heating (30 s ramp heating to 600–650 °C). Any unconverted Hg^{II} released during Au cartridge heating is either re-adsorbed on tubing downstream of the Au cartridge, or passes undetected through the Tekran analyzer since CVAFS only detects Hg⁰ [14,25]. Quantitative thermal reduction of Hg^{II} to Hg⁰ requires specific conditions: HgII is usually reduced by direct introduction into thermolyzers maintained at constant temperatures >600 °C [17,29,33] and/or with the aid of thermal reduction catalysts, such as aluminum oxide [18] or quartz wool [33]. The thermal reduction of Hg^{II} is particularly challenging when ramp heating of sorbent materials (such as Au sorbents) is used, as the occurrence of thermal reduction inefficiency is common [18].

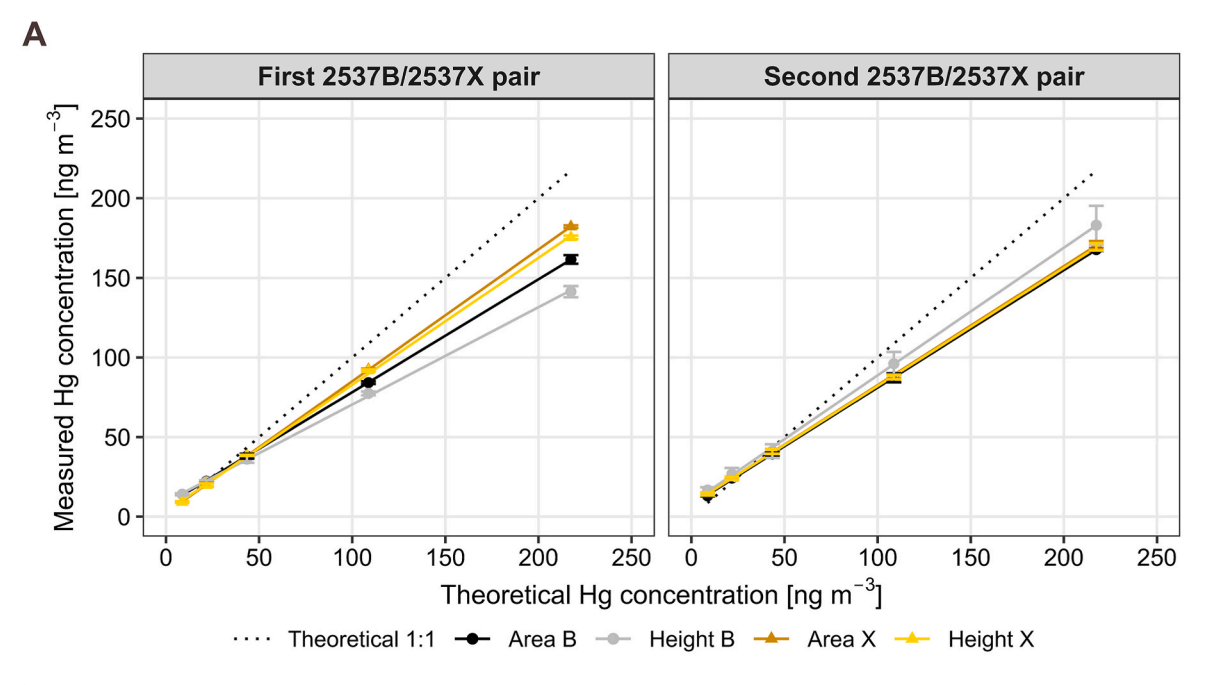
Fig. 4C shows the results of Hg^{II} injection into the thermolyzer upstream of the Tekran analyzer. The mean Hg^{II} recovery was 97 % \pm 14 % (mean \pm SD). The standard deviation was relatively high due to the logistics of the calibrator-thermolyzer connection. The calibrator outlet had to be as close as possible to the thermolyzer inlet, while also being far enough to prevent possible desorption of Hg into the sampling line due to elevated temperatures. On the other hand, if the calibrator outlet was too far from the thermolyzer, adsorption losses of Hg^{II} were observed. Nevertheless, it is clear that the obtained recovery values were higher compared to tests without the use of a thermolyzer.

The recovery of Hg^{II} measured as Au cartridge breakthrough onto CEM was below the limit of detection for all conducted tests (<10 pg, n = 10; 99 % collection efficiency). Insignificant breakthrough values for Au cartridge Hg^{II} sampling indicate that Au cartridges quantitatively retain Hg^{II} .

Based on the Au sampling results, the implications for atmospheric Hg measurements using Tekran 2537 analyzers are as follows: i) the analyzer measures an atmospheric Hg fraction somewhere between gaseous Hg⁰ and TGM; ii) Hg^{II} is not measured quantitatively due to adsorption losses of HgII on surfaces inside the analyzer, and due to incomplete thermal reduction of Hg^{II} to Hg^0 during the Au cartridge heating; iii) a thermolyzer can be used upstream of the analyzer to allow TGM measurement due to minimization of adsorption losses and quantitative thermal reduction of Hg^{II} to Hg⁰; and iv) Au cartridges retain Hg^{II} efficiently under laboratory conditions, with no quantifiable breakthrough under the experimental conditions. These implications may be generalized for all analyzers and manual methods that sample and measure atmospheric Hg using Au sorbent materials. However, since this study focused on tests with gaseous HgBr2, future research should incorporate calibrators based on the permeation of other atmospherically relevant Hg^{II} compounds, following a similar experimental design.

3.3. Comparison of peak integration types and Tekran 2537 analyzer models

The results of the comparison are shown in Fig. 5. The theoretical 1:1 line was obtained adjusting the results to the calibration curve obtained



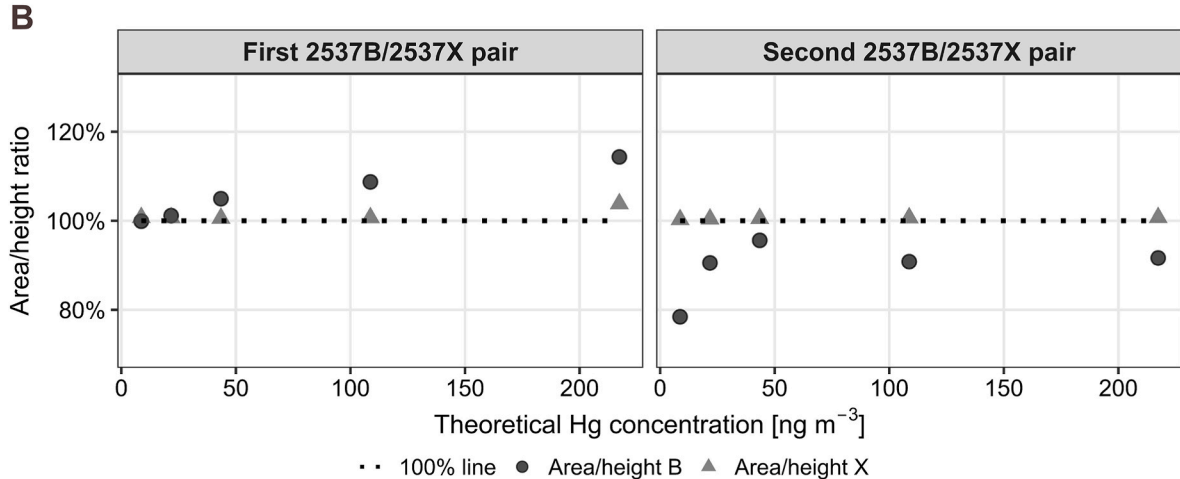


Fig. 5. Comparison of peak integration types (peak area and peak height) and Tekran 2537 analyzer models (2537B and 2537X) using the Hg⁰ permeation calibrator for A) the first pair of Tekran 2537 analyzers and B) the second pair of Tekran 2537 analyzers.

by bell jar Hg^0 injections and the Dumarey equation [22]. Theoretical Hg concentration for the Hg^0 permeation calibrator was obtained from the known permeation rate of the Hg^0 calibrator (10.9 \pm 0.7 pg s⁻¹, based on gravimetric measurements [19]).

The slopes of ordinary least squares (OLS) regressions differed between peak integration types, Tekran 2537 analyzer models, and also between different pairs of instruments (OLS regression slopes, intercepts, standard errors, and r² values are shown in Table S2). The most consistent trend was that the Hg⁰ concentrations measured using the Tekran 2537B and Tekran 2537X analyzers were lower than expected, for both analyzer pairs and for both peak height and peak area integrations, indicating the problem of incomparable calibration methods. There are disagreements about the Dumarey equation, which describes the temperature dependence of saturated Hg⁰ vapor concentration in the bell jar. Some publications have shown that the Dumarey equation gives accurate Hg⁰ concentrations [34,35], while others have noted discrepancies, but do not provide an alternative [36-39]. Relative differences of 15 % (first Tekran 2537B), 5 % (second Tekran 2537B), −0.5 % (first Tekran 2537X), and 4 % (second Tekran 2537X) were observed between bell jar calibrations and permeation calibrator calibrations (calibrator was taken as the reference for calculating relative differences, as shown

in equations (2)–(4)); the mean across all analyzers was 5.8 % \pm 7.0 % (mean \pm SD). The relative difference of 5.8 % implies that measurements calibrated using the bell jar and the Dumarey equation will result in atmospheric Hg concentrations 5.8 % lower than measurements calibrated using the calibrator. This value is in agreement with underestimations reported by Huber et al. [38] (7 %), Quétel et al. [39] (5.8 %), and de Krom et al. [40] (8 %). However, the large variability (7.0 % SD) between different Tekran 2537 analyzers suggests that the value observed in our work should be taken with caution.

The OLS regression intercepts were significantly different from zero for all regressions (p < 0.05) and most were high enough to lead to bias if the calibration curves were extrapolated to the ambient air measurement range (Table S2). On the other hand, forcing intercepts to zero, as is done for automated internal calibrations of the 2537 instruments, could also bias ambient air measurements if a real non-zero intercept exists. Bell jar and calibrator Hg^0 injections in this study all occurred at concentrations well above ambient levels. Precise, traceable calibrations in the ambient range are needed to ensure no bias exists in ambient air Hg measurements, as have been carried out by Andron et al. [34].

Hg⁰ concentrations measured with the Tekran 2537X analyzers were higher than for the 2537B and closer to the theoretical 1:1 line in all

cases, except for the second 2537B/2537X pair and peak area integration in Fig. 5A. The comparison of the two different Tekran 2537 analyzer models reveals that the difference between analyzer models was not statistically significant (Friedman, p > 0.05) in all cases, except when comparing the peak area integration of 2537B and 2537X for the second pair of instruments (Fig. 5A). However, it is important to note that using only the internal ${\rm Hg}^0$ permeation source of the Tekran analyzers for calibration instead of the bell jar multipoint calibration curve, the results between analyzers were significantly different for both analyzer pairs and both integration types (Fig. S3; Friedman, p < 0.05). This illustrates the importance of performing a multipoint calibration curve for atmospheric Hg measurements, as the comparability of the obtained results was greatly compromised if only the internal calibration of the Tekran 2537 analyzers was used. The internal calibration uses a single loading of Hg^0 from a permeation source built into the analyzer [7]; typically, the loaded Hg⁰ from the internal permeation source greatly exceeds concentrations typical of ambient Hg concentrations. While single-point calibration is faster and requires less workload, it can introduce biases; multipoint calibration is generally superior in terms of accuracy and precision [41].

Looking at the difference between peak integration types (Fig. 5B), the difference between peak area and peak height integration for the Tekran 2537X analyzers was statistically significant (*t*-test, p<0.05); however, very small (mean area/height ratio of 101 ± 1 %). For Tekran 2537B analyzers, the difference due to peak integration type was greater and statistically significant (*t*-test, p<0.05), although the results were inconsistent between the two different 2537B analyzers. One 2537B analyzer gave higher Hg concentration results when using peak area integration (mean area/height ratio of 106 ± 6 %, Fig. 5B), while the other gave higher results when using peak height integration (mean area/height ratio of 89.4 ± 6 %, Fig. 5B).

The results for the comparison of Tekran analyzer models and Hg⁰ sources imply that: i) the difference in measured Hg concentration between peak height and peak area integration is negligible for Tekran 2537X models and considerable for Tekran 2537B models; ii) multipoint calibration curves at atmospherically relevant Hg concentrations are necessary to improve data comparability and accuracy of atmospheric Hg measurements, since internal single-point calibration of Tekran 2537 can be insufficient; and iii) on average, a 5.8 % underestimation of Hg concentration was observed for the bell jar calibration and the Dumarey equation based on comparisons with the Hg⁰ permeation calibrator, though the value was variable between different Tekran 2537 analyzers.

4. Conclusions

Stable and reproducible permeation rates of HgII together with a low ${\rm Hg^0/Hg^{II}}$ ratio were demonstrated for the ${\rm Hg^{II}}$ permeation calibrator used in our work. The results obtained with ${\rm Hg^0}$ and ${\rm Hg^{II}}$ permeation calibrators showed that improvements in Hg⁰ and Hg^{II} sources can uncover limitations and contribute to a better understanding of atmospheric Hg measurements using gold sampling. Au sampling and tests using the Tekran analyzer for atmospheric Hg revealed that the analyzer measures an atmospheric Hg fraction somewhere between gaseous Hg^0 and TGM due to Hg^{II} adsorption losses and inefficient Hg^{II} to Hg⁰ conversion during ramp heating of the Au cartridge. This is important since Hg^{II} concentrations can be up to ~ 25 % of ambient air concentrations, and higher in highly polluted areas and the marine boundary layer. Obtained outcomes can be extended to all atmospheric Hg analyzers and manual methods that apply Au sorbents for sampling and analysis, although further testing on specific Au sorbent analyzers and analyzers are needed. The comparison of atmospheric Hg analyzers revealed that calibration curves differ not only between different Tekran 2537 analyzers, but also between different calibration methods (e.g., bell jar and permeation calibrator). This highlights the importance of proper calibration, especially since even small relative changes in atmospheric Hg concentrations (<5 %) are considered significant for the Hg

biogeochemical cycle.

To promote the worldwide comparability of atmospheric Hg measurement data and the effectiveness evaluation of the Minamata Convention, the following recommendations are proposed for future atmospheric Hg measurements.

- 1) For atmospheric Hg analyzers utilizing gold trap preconcentration:
 - Cation-exchange membranes (removal of Hg^{fl}) should be used upstream of the sample line for gaseous Hg⁰ measurement.
 - Thermolyzers (Hg^{II} to Hg⁰ conversion) should be used upstream of the sample line for TGM measurement.
 - Minimization of surface area (sample line length, upstream filters for particulates) to eliminate Hg^{II} adsorption losses when measuring TGM.
- The use of multipoint calibration that provides more accurate and precise results in comparison to single-point calibration for atmospheric Hg measurements.
- The use of well-characterized mercury calibrators that are traceable to the International System of Units to ensure the comparability of results.

CRediT authorship contribution statement

Jan Gačnik: Writing – original draft, Visualization, Validation, Investigation, Data curation, Conceptualization. Seth Lyman: Writing – review & editing, Software, Project administration, Funding acquisition. Sarrah M. Dunham-Cheatham: Writing – review & editing, Methodology, Investigation, Data curation. Mae Sexauer Gustin: Writing – review & editing, Project administration, Funding acquisition, Conceptualization.

Declaration of competing interest

The authors declare that they have no known competing financial interests or personal relationships that could have appeared to influence the work reported in this paper.

Data availability

Data will be made available on request.

Acknowledgements

Funding for the project came from the National Science Foundation Division of Atmospheric & Geospace Sciences, grant numbers 2043042, 1951513, and 2044537. Thanks to the undergraduate student research assistants that work in the Gustin lab that keep the glassware clean and help with lots of things: Mitch Aikin, Nicole Choma, Abi Connolly, Chris Ford, Ryan Murphy, and Morgan Yeager. Trevor O'Neil, a research technician at USU, and Tyler Elgiar, Davis Smuin, Jackson Liesik, Rachel Merrill, and KarLee Zager, student researchers at Utah State University participated in construction and testing of calibrators and permeation tubes. The authors would also like to acknowledge the users Creative Pixa and Ylivdesign for providing copyright-free PNG artwork (available at www.pngtree.com) that was used in part to make the graphical abstract and Fig. 2. We thank the three anonymous reviewers for their valuable feedback.

Appendix A. Supplementary data

Supplementary data to this article can be found online at https://doi.org/10.1016/j.aca.2024.342956.

References

- [1] W.E. Brooks, H. Öztürk, Z. Cansu, Amalgamation and small-scale gold mining at ancient sardis, Turkey, Archaeological Discovery 05 (2017) 42–59, https://doi. org/10.4236/ad.2017.51003.
- [2] R.A. Carr, J.B. Hoover, P.E. Wilkniss, Cold-vapor atomic absorption analysis for mercury in the Greenland Sea, Deep-Sea Res. Oceanogr. Abstr. 19 (1972) 747–752, https://doi.org/10.1016/0011-7471(72)90067-8.
- [3] J. Ólafsson, Determination of nanogram quantities of mercury in sea water, Anal. Chim. Acta 68 (1974) 207–211, https://doi.org/10.1016/S0003-2670(01)85163-1
- [4] S.H. Williston, Mercury in the atmosphere, J. Geophys. Res. 73 (1968) 7051–7055, https://doi.org/10.1029/eo065i025p00402-04.
- [5] S.K. Pandey, K.H. Kim, R.J.C. Brown, Measurement techniques for mercury species in ambient air, TrAC, Trends Anal. Chem. 30 (2011) 899–917, https://doi.org/ 10.1016/j.trac.2011.01.017.
- [6] S.N. Lyman, I. Cheng, L.E. Gratz, P. Weiss-Penzias, L. Zhang, An updated review of atmospheric mercury, Sci. Total Environ. 707 (2020) 135575, https://doi.org/ 10.1016/j.scitotenv.2019.135575.
- [7] Tekran Instruments Corporation, Model 2537B ambient mercury vapor analyzer user manual. Rev. 3 (2007) 10.
- [8] J.L. Ambrose, Improved methods for signal processing in measurements of mercury by Tekran ® 2537A and 2537B instruments, Atmos. Meas. Tech. 10 (2017) 5063–5073.
- [9] F. Slemr, A. Weigelt, R. Ebinghaus, H.H. Kock, J. Bödewadt, C.A. M. Brenninkmeijer, A. Rauthe-schöch, S. Weber, M. Hermann, J. Becker, A. Zahn, B. Martinsson, C. Mpic, Atmospheric mercury measurements onboard the CARIBIC passenger aircraft, Atmos. Meas. Tech. 9 (2016) 2291–2302, https://doi.org/ 10.5194/amt-9-2291-2016.
- [10] P.C. Swartzendruber, D.A. Jaffe, B. Finley, Improved fluorescence peak integration in the Tekran 2537 for applications with sub-optimal sample loadings, Atmos. Environ. 43 (2009) 3648–3651, https://doi.org/10.1016/j.atmosenv.2009.02.063.
- [11] M. Gustin, D. Jaffe, Reducing the uncertainty in measurement and understanding of mercury in the atmosphere, Environ. Sci. Technol. 44 (2010) 2222–2227, https://doi.org/10.1021/es902736k.
- [12] M.S. Gustin, J. Huang, M.B. Miller, C. Peterson, D.A. Jaffe, J. Ambrose, B.D. Finley, S.N. Lyman, K. Call, R. Talbot, D. Feddersen, H. Mao, S.E. Lindberg, Do we understand what the mercury speciation instruments are actually measuring? Results of RAMIX, Environ. Sci. Technol. 47 (2013) 7295–7306, https://doi.org/10.1021/es3039104.
- [13] F. Slemr, E.G. Brunke, R. Ebinghaus, J. Kuss, Worldwide trend of atmospheric mercury since 1995, Atmos. Chem. Phys. 11 (2011) 4779–4787, https://doi.org/ 10.5194/acp-11-4779-2011.
- [14] S.J. Long, D.R. Scott, R.J. Thompson, Atomic absorption determination of elemental mercury collected from ambient air on silver wool, Anal. Chem. 45 (1973) 2227–2233, https://doi.org/10.1021/ac60335a032.
- [15] S.M. Dunham-Cheatham, S. Lyman, M.S. Gustin, Comparison and calibration of methods for ambient reactive mercury quantification, Sci. Total Environ. 856 (2023) 159219, https://doi.org/10.1016/j.scitotenv.2022.159219.
- [16] S. Lyman, C. Jones, T. O'Neil, T. Allen, M. Miller, M.S. Gustin, A.M. Pierce, W. Luke, X. Ren, P. Kelley, Automated calibration of atmospheric oxidized mercury measurements, Environ. Sci. Technol. 50 (2016) 12911–12927, https://doi.org/ 10.1021/acs.est.6b04211.
- [17] S.N. Lyman, L.E. Gratz, S.M. Dunham-cheatham, M.S. Gustin, A. Luippold, Improvements to the accuracy of atmospheric oxidized mercury measurements, Environ. Sci. Technol. 54 (2020) 13379–13388, https://doi.org/10.1021/acs.est.0c02747.
- [18] J. Gačnik, I. Živković, S. Ribeiro Guevara, J. Kotnik, S. Berisha, S. Vijayakumaran Nair, A. Jurov, U. Cvelbar, M. Horvat, Calibration approach for gaseous oxidized mercury based on nonthermal plasma oxidation of elemental mercury, Anal. Chem. 94 (2022) 8234–8240, https://doi.org/10.1021/acs.analchem.2c00260.
- [19] T.R. Elgiar, S.N. Lyman, T. O'Neil, J. Gačnik, S.M. Dunham-Cheatham, M.S. Gustin, A NIST-Traceable Dilution Calibrator for Oxidized Mercury. in preparation, (n.d.).
- [20] M.B. Miller, S.M. Dunham-Cheatham, M.S. Gustin, G.C. Edwards, Evaluation of cation exchange membrane performance under exposure to high Hg0 and HgBr2 concentrations, Atmos. Meas. Tech. 12 (2019) 1207–1217, https://doi.org/ 10.5194/amt-12-1207-2019.
- [21] N. Allen, J. Gačnik, S.M. Dunham-Cheatham, M.S. Gustin, Interaction of reactive mercury with surfaces and implications for atmospheric mercury speciation measurements, Atmos. Environ. 318 (2024) 120240, https://doi.org/10.1016/j. atmosphy. 2023. 120240.

- [22] R. Dumarey, Comparison of the collection and desorption efficiency of activated charcoal, silver, and gold for the determination of vapor-phase atmospheric mercury, Anal. Chem. 57 (1985) 2644–2646.
- [23] R.J.C. Brown, A.S. Brown, Accurate calibration of mercury vapour measurements, Analyst 133 (2008) 1611–1618, https://doi.org/10.1039/b806860g.
- [24] Y. Tang, S. Wang, G. Li, D. Han, K. Liu, Z. Li, Q. Wu, Elevated gaseous oxidized mercury revealed by a newly developed speciated atmospheric mercury monitoring system, Environ. Sci. Technol. 56 (2022) 7707–7715, https://doi.org/ 10.1021/acs.est.2c01011.
- [25] U.S. Environmental Protection Agency, EPA method 1631, revision E: mercury in water by oxidation. Purge and Trap, and Cold Vapor Atomic Fluorescence, Revision E, 2002, p. 38.
- [26] R Core Team, R, A Language and Environment for Statistical Computing, 2021.
- [27] M. Davis, J. Lu, Calibration sources for gaseous oxidized mercury: a review of source design, performance, and operational parameters, Crit. Rev. Anal. Chem. (2022), https://doi.org/10.1080/10408347.2022.2131373.
- [28] X. Feng, S. Tang, L. Shang, H. Yan, J. Sommar, O. Lindqvist, Total gaseous mercury in the atmosphere of Guiyang, PR China, Sci. Total Environ. 304 (2003) 61–72, https://doi.org/10.1016/S0048-9697(02)00557-0.
- [29] C.P. Jones, S.N. Lyman, D.A. Jaffe, T. Allen, T.L. O'Neil, Detection and quantification of gas-phase oxidized mercury compounds by GC/MS, Atmos. Meas. Tech. 9 (2016) 2195–2205, https://doi.org/10.5194/amt-9-2195-2016.
- [30] J. Gačnik, I. Živković, S. Ribeiro Guevara, R. Jaćimović, J. Kotnik, M. Horvat, Validating an evaporative calibrator for gaseous oxidized mercury, Sensors 21 (2021) 2501, https://doi.org/10.3390/s21072501.
- [31] G.R. Sheu, R.P. Mason, An examination of methods for the measurements of reactive gaseous mercury in the atmosphere, Environ. Sci. Technol. 35 (2001) 1209–1216, https://doi.org/10.1021/es001183s.
- [32] M.S. Gustin, H.M. Amos, J. Huang, M.B. Miller, K. Heidecorn, Measuring and modeling mercury in the atmosphere: a critical review, Atmos. Chem. Phys. 15 (2015) 5697–5713, https://doi.org/10.5194/acp-15-5697-2015.
- [33] M.S. Gustin, S.M. Dunham-Cheatham, L. Zhang, Comparison of 4 methods for measurement of reactive, gaseous oxidized, and particulate bound mercury, Environ. Sci. Technol. 53 (2019) 14489–14495, https://doi.org/10.1021/acs. est.9b04648.
- [34] T.D. Andron, W.T. Corns, I. Živković, S.W. Ali, S. Vijayakumaran Nair, M. Horvat, Traceable and continuous flow calibration method for gaseous elemental mercury at low ambient concentrations, Gases/Laboratory Measurement/Validation and Intercomparisons (2023). https://doi.org/10.5194/amt-2023-169.
- [35] R. Dumarey, R.J.C. Brown, W.T. Corns, A.S. Brown, P.B. Stockwell, Elemental mercury vapour in air: the origins and validation of the "Dumarey equation" describing the mass concentration at saturation, Accred Qual. Assur. 15 (2010) 409–414. https://doi.org/10.1007/s00769-010-0645-1.
- 409–414, https://doi.org/10.1007/s00769-010-0645-1.
 [36] I. de Krom, W. Bavius, R. Ziel, E. Efremov, D. van Meer, P. van Otterloo, I. van Andel, D. van Osselen, M. Heemskerk, A.M.H. van der Veen, M.A. Dexter, W. T. Corns, H. Ent, Primary mercury gas standard for the calibration of mercury measurements, Measurement: Journal of the International Measurement Confederation 169 (2021) 108351, https://doi.org/10.1016/j.measurement.2020.108351.
- [37] A. Srivastava, J.T. Hodges, Development of a high-resolution laser absorption spectroscopy method with application to the determination of absolute concentration of gaseous elemental mercury in air, Anal. Chem. 90 (2018) 6781–6788, https://doi.org/10.1021/acs.analchem.8b00757.
- [38] M.L. Huber, A. Laesecke, D.G. Friend, Correlation for the vapor pressure of mercury, Ind. Eng. Chem. Res. 45 (2006) 7351–7361, https://doi.org/10.1021/ ie0605608
- [39] C.R. Quétel, M. Zampella, R.J.C. Brown, H. Ent, M. Horvat, E. Paredes, M. Tunc, International system of units traceable results of Hg mass concentration at saturation in air from a newly developed measurement procedure, Anal. Chem. 86 (2014) 7819–7827, https://doi.org/10.1021/ac5018875.
- [40] I. De Krom, W. Bavius, R. Ziel, E.A. Mcghee, R.J.C. Brown, I. Živković, J. Gačnik, V. Fajon, J. Kotnik, M. Horvat, H. Ent, Comparability of calibration strategies for measuring mercury concentrations in gas emission sources and the atmosphere, Atmos. Meas. Tech. 14 (2021) 2317–2326, https://doi.org/10.5194/amt-14-2317-2021.
- [41] M.M. Khamis, N. Klemm, D.J. Adamko, A. El-Aneed, Comparison of accuracy and precision between multipoint calibration, single point calibration, and relative quantification for targeted metabolomic analysis, Anal. Bioanal. Chem. 410 (2018) 5899–5913, https://doi.org/10.1007/s00216-018-1205-5.